

## **MODERN TECHNIQUES IN X-RAY DIFFRACTION-APPLIED TO METALLURGY**

**Johan de Villiers  
Sabine Verryn  
University of Pretoria**

### **Abstract**

Through the application of the Rietveld method, X-ray diffraction analysis has developed into a fully quantitative method for phase analysis. The Rietveld method itself has progressed from an unstable method that required constant operator intervention to a stable and robust method suited even for routine analysis. The method however, requires a good initial calibration and periodic checks on its precision and accuracy.

Several examples from minerals processing, pyrometallurgy, and materials science show the strengths and applicability of the method. The limitations and sources of error are also discussed.

### **1. Introduction**

Diffraction of X-rays by matter has been used for more than 80 years, initially to elucidate the structure of crystalline matter, and to investigate the bonding between atoms. The first development of powder diffraction cameras and the later development of X-ray diffractometers saw the development of methods to identify phases and to try to quantify them in mixtures. A comprehensive database and search-match techniques have been developed over the ensuing years.

Effective and accurate quantification had to wait for the so-called Rietveld<sup>1</sup> analysis where the total diffraction pattern is used and where the crystal structure data for the constituent phases are needed as input. Overlapping of diffraction peaks of different phases is handled without difficulty and reliable results can be obtained in spite of this occurrence.

The development of methods for structure analysis from powder data has also progressed rapidly and more and more complex structures are being solved from first principles, i.e. without knowledge of unit cell or space group data.

Because of the ease of use of the Rietveld method, it is finding increased application in metallurgy, especially in the quantification of phases of importance in minerals processing, in pyrometallurgical processes, and in materials characterization. This study will examine the principles of the Rietveld method, its application in metallurgy, and finally also the common pitfalls that need to be avoided.

### **2. Rietveld Analysis**

As the Rietveld method compares the experimental diffraction pattern with one calculated from known crystal structure data, the following data are needed:

- An XRD Pattern with as low a background as possible. This should have good resolution and high diffraction peak intensities. With modern X-ray detectors, this can be achieved in minutes rather than hours.
- Instrumental parameters such as goniometer radii and slit sizes are needed. These are the so-called "Fundamental parameters". They are used to calculate the shapes of the resultant diffraction peak profiles that are caused by the instrument. The parameters are used to correctly separate the instrumental effects on the diffraction pattern from the sample effects.

- Phase specific parameters are needed for every phase that is present in the sample. These are the unit cell and space group, atomic parameters and preferably, the compositions of solid solution phases (spinel, silicates, etc.).

The Rietveld method is based on a least squares fit of the experimental data to a calculated pattern in which all the known phases are included. Initially, the method used analytic functions to describe the diffraction peak shapes and the method was very unstable, requiring constant operator intervention. The more modern software has greatly improved the stability and the peak profiles are now calculated from first principles, giving much better descriptions of the measured peak profiles. Table 1 shows the essential data needed to calculate the diffraction pattern of pseudobrookite, the main phase in titania slags.

Crystal Data:  $\text{FeTi}_2\text{O}_5$

Unit cell data:  $a = 3.769\text{\AA}$   $b = 9.765\text{\AA}$   $c = 9.987\text{\AA}$   $\alpha = \beta = \gamma = 90^\circ$

Unit cell volume:  $367.564 \text{\AA}^3$

Space Group:  $Cmcm$

Atomic position parameters:

Atom	x	y	z	Atoms/Cell
Fe	0	0.8093	$\frac{1}{4}$	4
Ti	0	0.1335	0.0623	8
O1	0	0.2316	$\frac{1}{4}$	4
O2	0	0.0408	0.8900	8
O3	0	0.3163	0.9379	8

Table 1. Crystal data for  $\text{M}_3\text{O}_5$

Figure 1(a) shows the unit cell with the atoms as specified in the so-called asymmetric unit, as well as the contents of the full unit cell as a result of applying the symmetry of the space group. This is the used to calculate the full diffraction pattern of the  $\text{M}_3\text{O}_5$  phase (using the freeware programme Powdercell<sup>2</sup>, shown in Figure 2).

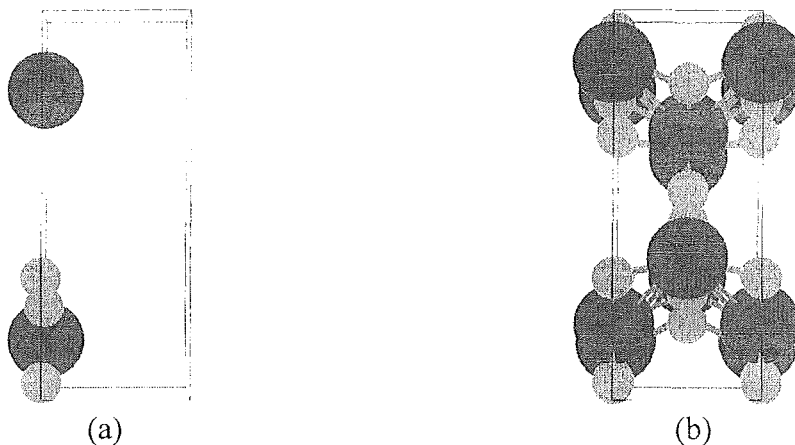


Figure 1. (a) The positions of the atoms in the asymmetric unit, and (b) the positions of the atoms in the unit cell, after applying the symmetry of the space group.

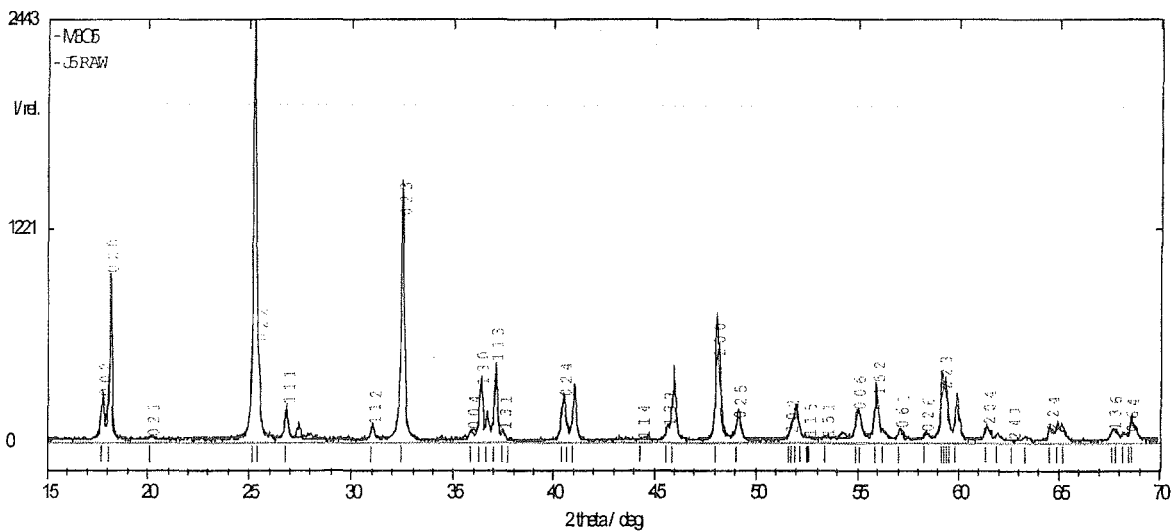


Figure 2. Calculated (red) and observed (black) X-ray diffraction pattern of  $M_3O_5$ . The fundamental formula to calculate the mass fraction of every phase in a mixture is<sup>3</sup>:

$$W_p = \frac{S_p(ZMV)_p}{\sum_{i=1}^n S_i(ZMV)_i}$$

Z is the number of formula units in the unit cell, M is the mass per formula unit, and V is the volume of the unit cell. S is the scale factor as determined by least squares fitting of the measured and calculated X-ray diffraction patterns.

### 3. Calibration

The diffraction pattern is a folding or convolution of the X-ray source profile, the instrument factors, and the sample factors. This can be written as<sup>4</sup>:

$$Y(2\theta) = (W \times G) \times S$$

Where W represents the contribution of the source profile to the observed diffraction pattern, G represents the instrumental contribution (geometry, slits, etc.), and S represents the sample contribution (which we would like to separate from the other effects).

Calibration of the instrument and its diffraction pattern is usually done by carefully collecting the XRD data of a well-characterised cubic compound of which all the parameters except the instrument parameters are known. The instrument parameters can then be easily determined and then these can be kept invariant till the instrument is re-aligned. It is essential that a good fit be obtained. This is indicated by the so-called weighted R-factor or discrepancy factor. The term  $y_i$  is the intensity of the  $i^{\text{th}}$  step in the diffraction pattern.

$$R_{wp} = \left\{ \frac{\sum w_i (y_i(\text{obs}) - y_i(\text{calc}))^2}{\sum w_i (y_i(\text{obs}))^2} \right\}^{1/2} \quad (\text{'R-weighted pattern'})$$

Figure 3 shows the refinement and calibration of  $Y_2O_3$  giving an Rwp of 5% and also showing the difference between the observed and calculated profiles.

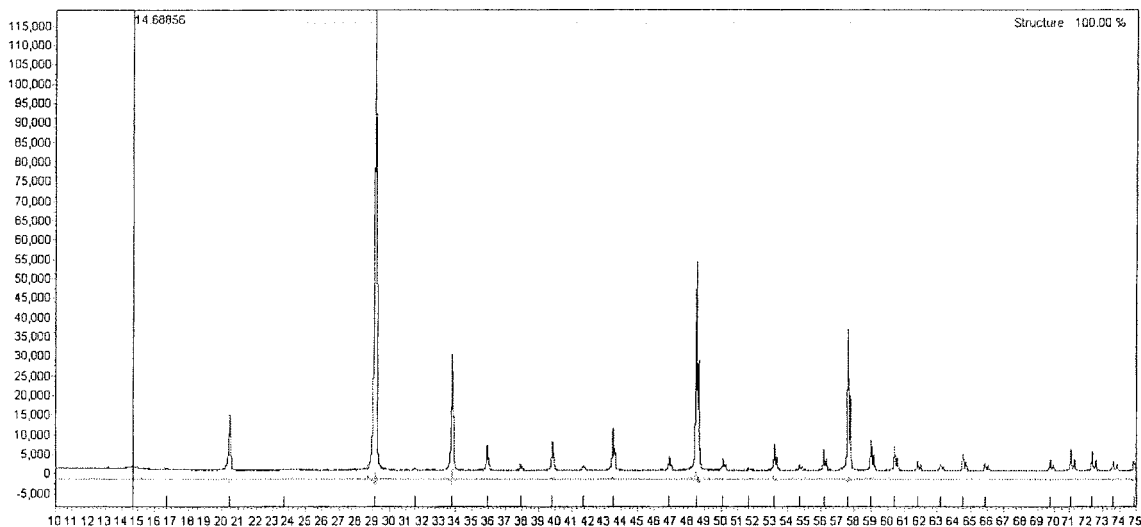


Figure 3. Fitted XRD pattern of  $Y_2O_3$ . The Rwp is 5%. Also shown below the pattern is the difference curve. This curve is almost featureless with small deviations only at the peak positions.

#### 4. Applications in metallurgy

##### 4.1 Ilmenite roasting

Ilmenite is paramagnetic, but when it is roasted it becomes antiferromagnetic and can be separated from chromite using magnetic separation. This is due to the formation of rutile so that the ilmenite becomes more iron-rich and thus more magnetic. The formation of iron-rich ilmenite-hematite solid solution can only be followed using XRD methods. This provides an easy and accurate method to establish the ideal roasting conditions. Figure 4 shows the refinement of a roasted ilmenite and its composition as determined using the curve given in Navrotsky and Nord<sup>5</sup>.

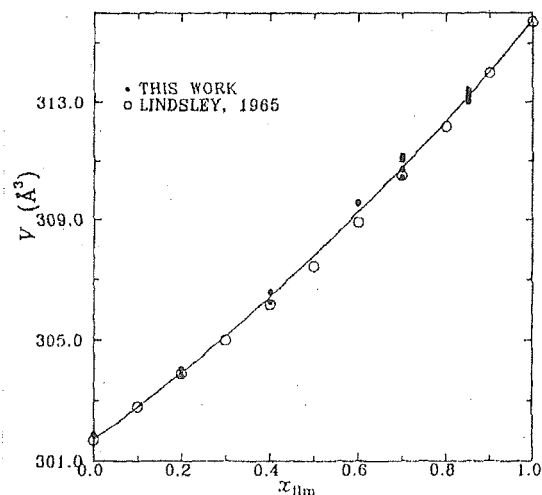
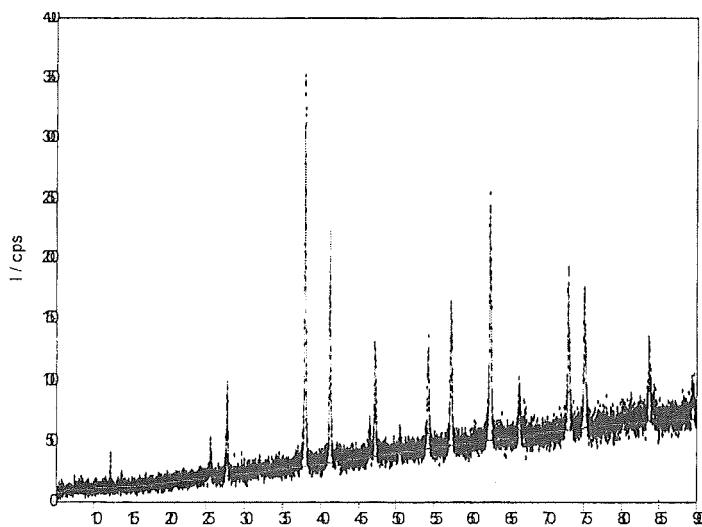


Figure 4. Refinement of the unitcell dimensions of ilmenite,  $a = 5.0843(2)\text{\AA}$ ,  $c = 13.9955\text{\AA}$ , with  $V = 313.3 \text{\AA}^3$ . This relates to the mole fraction of ilmenite in the  $\text{Fe}_2\text{O}_3\text{-FeTiO}_3$  solid solution,  $X_{\text{ilm}}=0.85$ .

#### 4.2 Analysis of SiC polytypes

The polytypism or stacking variation of silicon carbide has been studied for decades. Since all polytypes have the same composition, XRD, together with Raman spectrometry is widely used for the determination of the polytypes in commercial SiC refractories. The polytype, together with the  $\text{Si}_3\text{N}_4$  binding material seems to have a marked effect on the strength of the refractory. The five phases in the refractory can easily be quantified and related to the strength of the material.

#### 4.3 Titania slags

XRD has been used to monitor the oxidation in titania slags, especially with the formation of oxidation products such as rutile. Figure 5 shows the inverse correlation between the rutile content, as determined by XRD, and the  $\text{Ti}_2\text{O}_3$  content, determined by titration, for four slags.

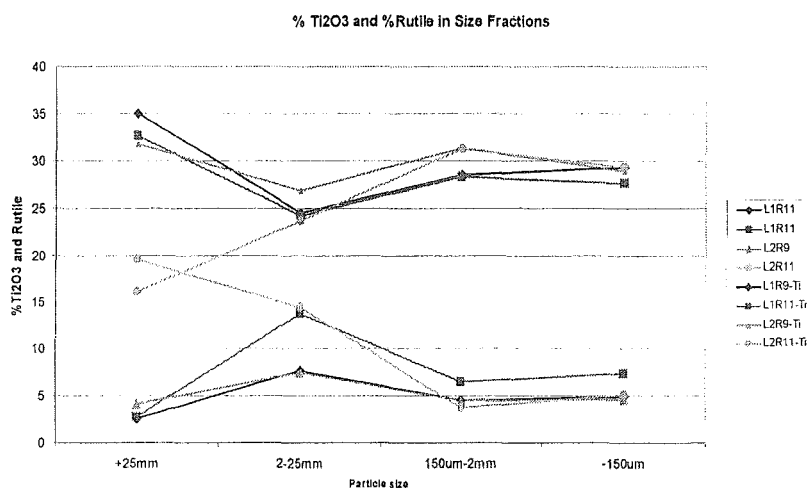


Figure 5. Variation in rutile and  $\text{Ti}_2\text{O}_3$  contents in titania slags

#### 4.4 Quantification of iron ore sinter phases

Iron ore sinter quality is strongly dependent on the presence of the so-called SFCA phase (silico-ferrite of iron and aluminium). This phase has previously been quantified using microscopic methods, and because of the inhomogeneity of the sinter, these methods are unreliable. Rietveld analysis can give very reproducible and reliable quantification of the major phases, including the SFCA. Figure 6 shows the result of an XRD quantification of a mechanical mixture of 15% hematite, 25% titaniferous magnetite, 15%  $\text{Ca}_2\text{SiO}_4$ , and 45% SFCA. The accuracy is excellent.

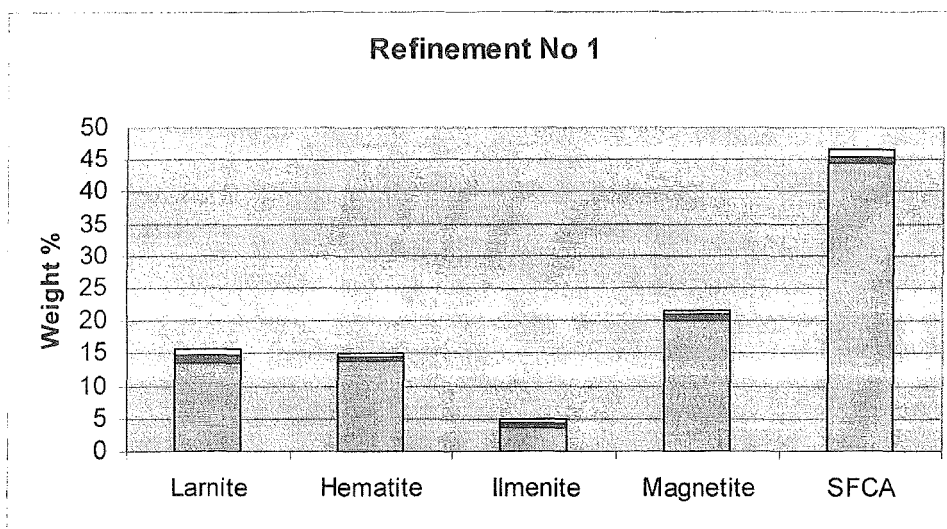


Figure 6. XRD quantification of phases occurring in iron ore sinters

#### 4.5 Talc and the effect of iron content

Talc is common gangue mineral that affects flotation of sulfides. It is hydrophobic, floats together with the sulfides, and often has to be depressed. The effect of various depressants is usually monitored by quantitative XRD analysis. This in turn, is affected by the chemistry of the talc. Figure 7 shows the effect of iron on the intensity of the main (111) talc peak.

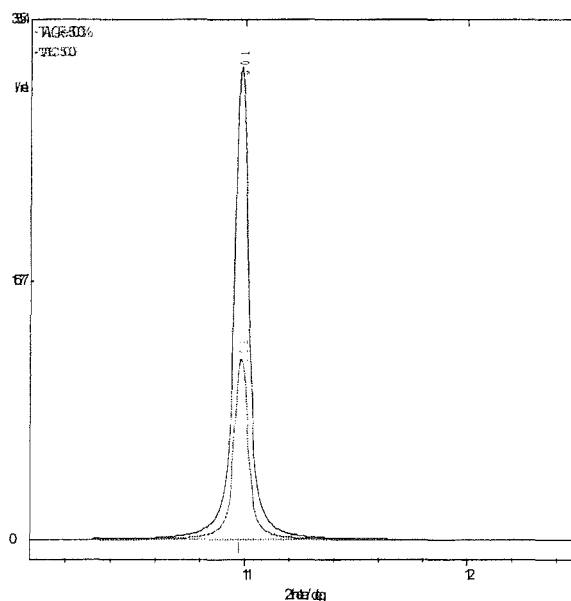


Figure 7. Peak intensity of an iron-containing talc (red), compared with a pure magnesium talc (blue).

#### 4.6 XRD at high temperatures

XRD has been used for the examination of the high-temperature behaviour of titania slags. Especially the oxidation behaviour leading to extensive disintegration has been examined at elevated temperature. Figure 8 shows

the variation of the cell dimensions with temperature, causing strain in the crystals, leading to cracking and disintegration.

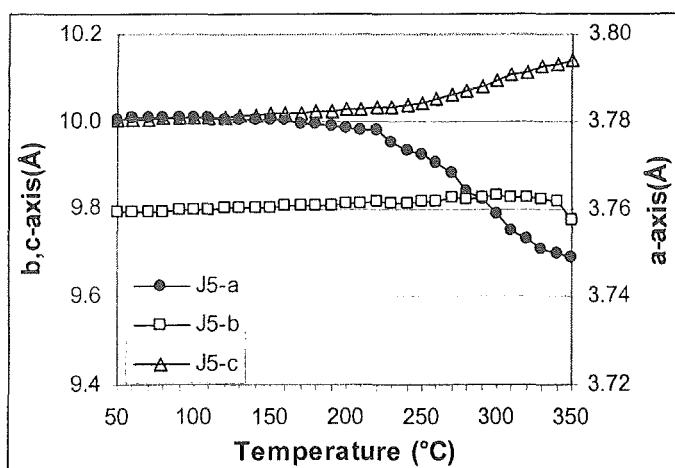


Figure 8. Changes in  $M_3O_5$  cell dimensions with temperature

### 5. Main sources of error

Mention must be made that Rietveld analysis is only as accurate as the quality of the data, and the calibration. Common sources of error are the following:

- Inadequate grinding leading to erroneous intensity data. This is the most common cause and care must be taken to adequately grind the sample to particle sizes less than 10-15 microns.
- Poor instrument alignment. This will result in poor instrument calibration with a large error even with standard samples. If this is the case, then poor results of other samples will also be produced.
- Inadequate identification of constituent phases. If all phases are not included in the refinement, then the results are meaningless.
- Chemical information of major solid solution phases is important for adequate quantification.
- Poorly crystalline samples such as expanding clays still remain a challenge to quantify.

### 6. Final comments

Modern XRD analysis has developed into a reliable method for the quantification of mineral and material phases. It can therefore provide important information of the mechanisms, and kinetics of metallurgical reactions. Processes can be better understood and modelled using XRD.

### 7. References.

1. Young, R A (ed) The Rietveld Method. IUCr . Oxford University Press, 298p
2. Powdercell – a program to visualize crystal structures, calculate the corresponding powder patterns and refine experimental curves. German Federal Centre for Materials Research and testing.
3. Hill, R J and Howard, C J (1987) Quantitative phase analysis from neutron powder diffraction data using the Rietveld method. J. Appl. Cryst. 20, 467-474.
4. Topas Users Manual, (2000) Copyright, BRUKER AXS GMBH.
5. Brown, N E, Navrotsky, A, Nord, G L, and Banerjee, S K, (1993) Hematite-Ilmenite ( $Fe_2O_3$ - $FeTiO_3$ ) solid solutions: Determinations of Fe-Ti order from magnetic properties.